Int J Adv Manuf Technol (2015) 77:1671–1679
DOI 10.1007/s00170-014-6574-0

ORIGINAL ARTICLE

Microstructural evolution and mechanical properties during the friction stir welding of 7075-O aluminum alloy

K. Dehghani · R. Ghorbani · A. R. Soltanipoor

Received: 24 October 2012 / Accepted: 2 November 2014 / Published online: 16 November 2014
© Springer-Verlag London 2014

Abstract In the present work, the AA7075-O was subjected to friction stir welding. The rotating and welding speeds were 630 rpm and 32 mm/min, respectively. The diameters of shoulder and pin were 30 and 5.7 mm, respectively. The length of threaded pin was 4.8 mm. The tensile, bending, and hardness tests were carried out on the friction stir-welded specimens. The results show that the strength of friction stir-welded sample was about 15 % (i.e., 25 MPa) higher than that of base metal. By contrast, the ductility of base metal was as much as twice that of friction stir-welded one. According to the obtained hardness profile, the maximum hardness was obtained for the stirred zone with a continuous decrease toward the base metal. This resulted in the formation of cracks after bending specimens prepared from weldment, while there was no sign of crack in the bent specimens taken from base metal. Besides, there are microstructural evolutions from the weldment toward the base metal. These include the variations in the size and distribution of precipitates. The precipitates were coarser in the heat-affected zone, while they were finer in the stirred zone.

K. Dehghani · R. Ghorbani (✉)
Department of Metallurgy and Mining Engineering,
Amirkabir University of Technology, Tehran, Iran
e-mail: reghmetal@gmail.com

K. Dehghani
e-mail: Dehghani@aut.ac.ir

K. Dehghani
Center of Excellence in Smart Materials and Dynamic Structures,
Amirkabir University of Technology, Tehran, Iran

A. R. Soltanipoor
Faraz Jossh Koosha Co., Isfahan, Iran
e-mail: a.soltanipoor@gmail.com

Keywords Friction stir welding · AA7075 · Mechanical properties

1 Introduction

The 7xxx series aluminum alloys are commonly used in the aircraft industry. However, as they are hardened via precipitation process, the presence of precipitates does not readily lend them to be joined by fusion welding [1]. Besides, the 7xxx aluminum alloys are generally classified as non-weldable materials because of improper solidified microstructure and the presence of porosities formed during conventional fusion welding. Consequently, the loss in the mechanical properties as compared to the base material is very significant. These factors make the joining of these alloys by conventional welding processes unattractive [2]. Therefore, friction stir welding (FSW) was used to weld the 7xxx aluminum alloys. For example, AA7075, which is considered as a non-weldable alloy by fusion processes, was joined by FSW [1]. The corrosion resistance of FSWed AA7075-T651 was investigated by Leonard [3]. Leonard [4] also characterized the microstructural evolution and aging behavior of FSWed AA7075-T651. He carried out the hardness testing to determine the response of the FSWed specimens to different aging times. Feng et al. [5] studied the microstructural changes and cyclic deformation of FSWed AA7075-T651. Su et al. [6] investigated the microstructural evolutions of friction stir-processed AA7075-T6 in different regions behind the pin tool. Mahoney et al. [7] studied the properties of FSWed AA7075 T651 via mechanical and microstructural investigations. Venugopal et al. [8] studied the microstructural changes, hardness properties, and corrosion behavior of AA7075-T6.

Despite a large number of investigations conducted on the properties of Al7075 joined by FSW [3–8], there is almost no work on the FSW of AA7075 with O temper. Almost all the

past works on the FSW of AA7075 are pertaining to T6 or T651 condition which exhibits the highest strength before welding. Therefore, the aim of present work was to perform the FSW on the AA7075-O as there was no report regarding the FSW of AA7075 in O temper.

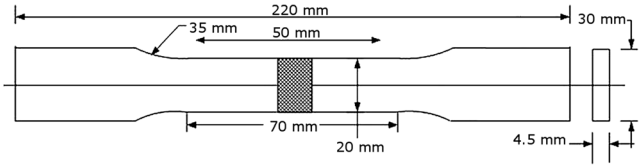

Fig. 1 Tensile test specimen

2 Experimental procedure

2.1 Material and FSW technique

The Al7075-O plates of 4.9-mm thickness were subjected to friction stir welding using a NC milling machine. The chemical composition of studied AA7075 is presented in Table 1. The used pin was H13 tool steel coated with a wear resistance nitride layer. The diameters of shoulder and pin were 30 and 5.7 mm, respectively. The length of threaded pin was 4.8 mm. Prior to welding, the butting faces of the plates were grounded and cleaned with methanol. The applied rotating and welding speeds were 630 rpm and 32 mm/min, respectively. The plunge depth was adjusted at 0.4 mm, whereas the tool angle was 2°. To provide sufficient heat required for welding, the workpiece was preheated to 100 °C. The temperature during FSW, measured using a pyrometer, was about 450±3 °C.

For microstructural observations, the specimens were prepared from four different regions: weldment, thermomechanically affected zone (TMAZ), heat-affected zone (HAZ), and base material. The microstructural evolutions were characterized using optical microscopy (OM) and scanning electron microscope (SEM) equipped with an energy-dispersive X-ray spectroscopy to analyze the phases.

It is worth mentioning that, as there were lot works on the effects of rotating and traverse speeds during the FSW of aluminum, we first did our research on the past works to choose the best or optimum amounts of FSW parameters for these alloys. Then, we carried out 16 FS welds under different conditions to confirm these amounts. Finally, we chose the best/optimum rotating and welding speeds of 630 rpm and 32 mm/min, respectively. In other words, to prevent repeating the past works and in order to be a new work, our aim was mainly to focus deeply on the microstructural evolutions and mechanical properties at a constant rotating and welding speeds. Thus, our goal was not to study the effects of different rotating and welding speeds, etc. However, at the constant rotating and welding speeds, we performed at least 16 FS welds required for preparing a lot of mechanical and microstructural studies. Then, to reach our goal, we carried out extensive mechanical tests (tensile, bending, hardness) and microstructural characterization (including SEM and OM).

2.2 Mechanical testing

Tensile specimens were prepared from the friction stir weld according to DIN 50123 (Fig. 1) [9]. The aim was to study the effects of microstructure zones, i.e., parent metal, HAZ, TMAZ, and weld nugget, on the mechanical properties of FSWed samples. Tensile tests were carried out at room temperature at a constant crosshead speed of 1 mm/min.

As for the bending test, dimensions of specimens were 20×220×4.5 mm^3. The bending test was carried out according to DIN 50121 [10]. Two types of bending test were carried out on the specimens prepared from FSWed workpiece. In the first method, the bending load was applied on the upper face of weldment, whereas in the second case, the weld root was subjected to the bending load. Bending load was employed at a speed of 10 mm/min.

With respect to the hardness, the Vickers hardness measurements were performed in the mid-thickness of FSWed samples using an applied load of 5 kg, as shown in Fig. 2. In order to obtain the hardness profile, the span between each measurement was 1.5 mm (Fig. 2).

In brief, for tensile testing, we performed at least six FS welds; thus, we carried out one tensile test for each weld. Besides, we did three tensile tests on the starting material to compare the results with welded conditions.

As for bending tests, again at least six FS welds were performed: three for testing on the root whereas the other three for testing on the face of welds. The same as tensile testing, three bending tests were carried out on the starting material to compare the results with welded conditions.

Table 1 The chemical composition of studied AA7075 (wt%)

Element	Zn	Mg	Cu	Si	Fe	Mn	Cr	Ni	Ti	Sn	Pb	Al
Percent	5.33	2.27	1.80	0.09	0.28	<0.03	0.19	<0.03	0.03	<0.03	<0.03	Balance

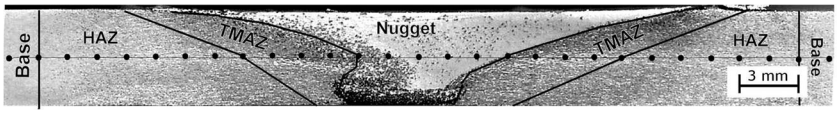

Fig. 2 Hardness measurements across the mid-thickness of FSWed sample

Regarding the hardness studies, we prepared the hardness profiles across the all welds. To obtain each profile, the harness measurements were carried out for at least 30 points/locations, as presented in Fig. 2. Even for each point, the measurement was carried out twice then the average was reported.

3 Results and discussion

3.1 Microstructural evolutions

Figure 3 illustrates the OM and SEM micrographs taken from the initial structure before FSW, while the SEM images taken from the microstructure of nugget and HAZ after FSW are presented in Fig. 4. The OM micrographs taken from the stir zone are shown in Fig. 5. Obviously, there are microstructural changes including the variations in the size and distribution of precipitates or second phases after FSW. The precipitates are relatively coarser in the HAZ and finer in the stirred zone.

According to the energy-dispersive X-ray spectroscopy (EDS) analyses presented in Fig. 6, the coarse particles (3–6 μm) are rich in Cu with the composition summarized in Table 2. Regarding the finer particles (smaller than 2 μm), they were identified as Al-Zn-Mg-Cu, i.e., rich in Zn, Mg, and Cu, with the compositions mentioned in Table 3. Referring to the EDS results shown in Fig. 7, they are most likely the η phase. According to the literature, this phase is $MgZn_2$, containing also AlCuM, $Mg(Zn,Al,Mg)_2$, and $Mg(Zn_2, AlMg)$ [11, 12].

As the dissolution temperature of η is within 300–350 °C [13], this phase can be therefore completely dissolved in the stirred zone [14], while it partially dissolves in the TMAZ. On the other hand, due to the short exposure time to high temperatures, it is possible that there is insufficient time for the complete dissolution of this phase. Therefore, there is another possibility that the coarse precipitates are broken up to much finer ones due to the characteristics of FSW. In this regard, it is reported that FSW can be a unique approach in modifying the as-cast and other structures by refining the coarse particles [15–22]. For example, Mehranfar and Dehghani [23] reported that the friction stir processing (FSP) of superaustenitic steels resulted in significant refining of sigma phases even to nanoscale. Thus, the refining of precipitates in nugget can be attributed to the breaking or shearing of coarse particles because of high strain rates dominated in the stir zone. In addition, although the re-precipitation of fine η phase can result in the enhancement of mechanical properties [22, 24, 25], it is far from happening during the short time of FSW. Thus, if it is supposed the re-precipitation occurs, these could be most likely Guinier–Preston (GP) and less likely η' whose formations take place during the early stages after solid solution treatment. However, this is out of the scope of present work, as it requires a more detailed study by TEM. Regarding the observed trend related to the hardness/strength, it should be considered that the GP and η' phases are mostly responsible for strengthening or age hardening but not η phase. Therefore, if the observed hardening was supposed to be due to η, the only possible mechanism is its breaking up or refining by FSW. That is why the nugget exhibited the highest hardness among the formed regions. As for the TMAZ, the structure refining by FSW in this region is less severe compared to the stirred zone. Consequently, as this region is less affected by FSW, the precipitates are coarser compared to stir zone (SZ) because their breaking up is less severe. However, they still are finer relative to those of base material. That is because some of the broken particles may also grow at the expense of

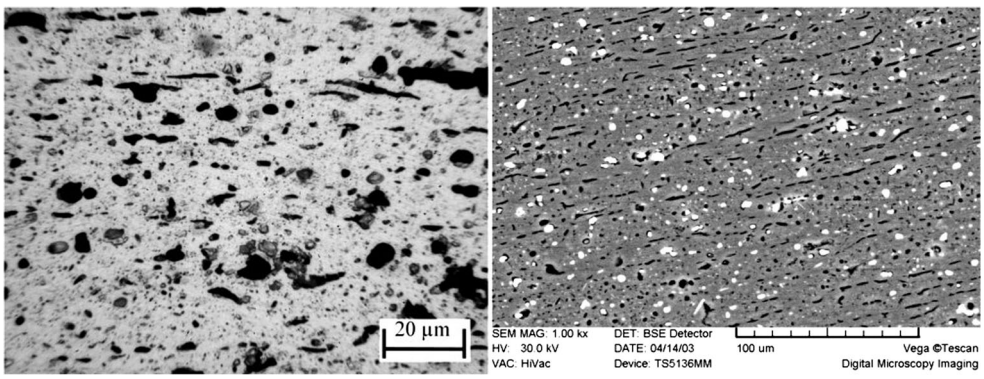

Fig. 3 OM and SEM images taken from the base metal

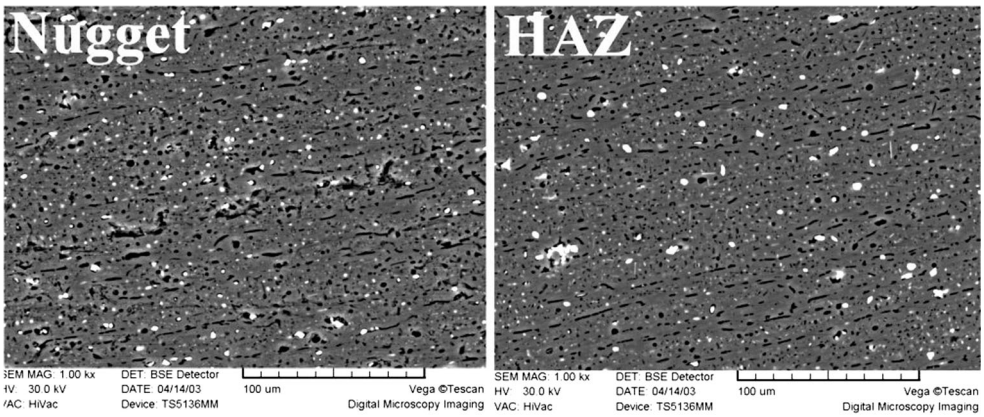

Fig. 4 SEM images taken from the weld nugget and HAZ

finer ones [14, 26]. With respect to the HAZ, there is no significant change in the precipitates size compared to base material. This resulted in almost identical hardness for base and HAZ since. This can be attributed to the traverse speed when the heat input was insufficient to make a noticeable change in the morphology and characteristics of particles which existed in the HAZ. The changes in particle size in different regions can be discussed in another way. That is, in the SZ, the dominant parameter is the strain rate resulting in the finer structure, whereas in the TMAZ, both strain rate and temperature are controlling factors but in a less effective way compared to SZ. In terms of HAZ, the only factor is temperature though its effect, as mentioned above, depends on the traverse speed. The role of temperature and strain rate in refining the microstructure during FSP of IF steel is well discussed in the recent work of authors [27]. With respect to the base material, the precipitates are affected neither by strain rate nor by temperature. As a result, the coarsest ones are formed in this zone, leading to the lowest hardness/strength.

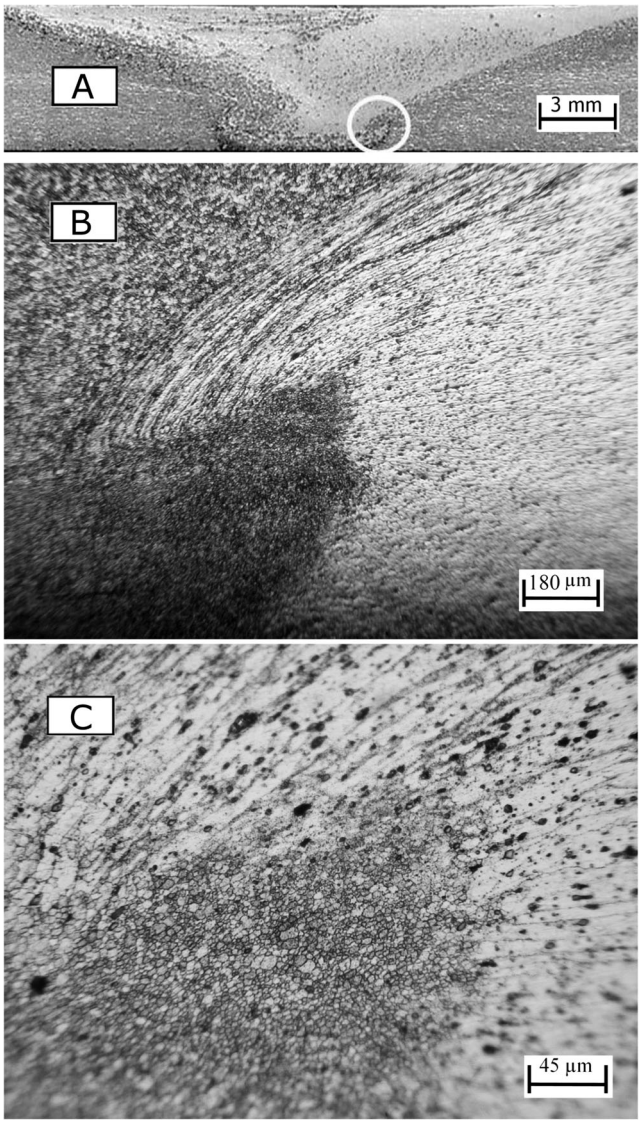

Fig. 5 The OM images taken from **a** the cross section of nugget and **b**, **c** region specified by circle magnified by ×50 and ×200, respectively

3.2 Hardness profile

The hardness profile obtained from the cross section of specimen subjected to FSW is presented in Fig. 8. Referring to this figure, the maximum hardness (150 Hv) is pertaining to the SZ or nugget. It is of interest that there is a two and half times increase in the hardness of weldment compared to that of base metal. As the starting material was in full-anneal condition (O temper), which exhibits the lowest hardness, such an increase in strength is not surprising. Thus, the deformation of coarse η precipitates to fine ones in SZ can be most likely responsible for the enhanced increase in hardness.

As the maximum hardness obtained in the present work is close to that of AA7075-T6 (175 Hv) [28], there could be another possibility regarding the highest strength in the SZ, that is, the dissolution of primary coarse particles followed by the reprecipitation of fine coherent phases in the SZ. This is in accordance with the findings of Uzun [22], Bussu et al. [24], and Starink et al. [25] who attributed the significant increase in strength and hardness to the fine dispersion of precipitates in the SZ. The re-precipitation after the dissolution of primary

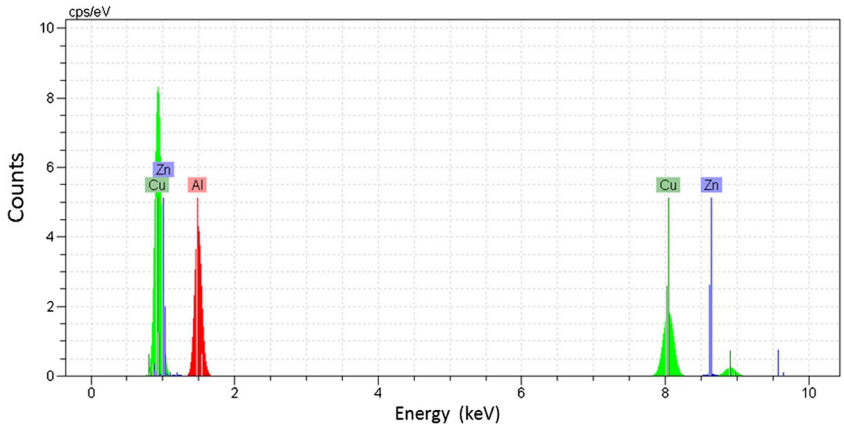

Fig. 6 EDS spectrum of the large precipitates

precipitates can take place according to the general precipitation sequence in AA7075 as follows [29, 30]:

$$\text{Solid solution} \rightarrow \text{GP zone} \rightarrow \text{metastable}\,\eta' \rightarrow \text{stable}\,\eta(MgZn_2) \quad (1)$$

However, the mentioned precipitation sequence may happen only in the SZ and partially in the TMAZ where the generated temperature is high enough to dissolve the primary precipitates followed by keeping the saturated solid solution to room temperature. However, if one assumes that the process of Eq. (1) can happen in the SZ and partially in TMAZ, then there could be no dissolution of primary phases and the re-precipitation of fine particles in the HAZ. That is why the precipitates in the HAZ are coarser compared to the SZ and TMAZ but finer relative to base material. Regarding the latter, as it is unaffected by the FSW, its microstructure does not change keeping the initial coarse precipitates existing in O-tempering condition.

Regarding the maximum strength in the nugget of FSWed specimen, it should be noted that the formation of GP zone and η' phase occurs at low-temperature aging of 20–120 °C [13]. Thus, although the precipitation sequence mentioned in Eq. (1) is far from happening during the present FSW, it is reported [14] that when the local concentration gradient is high, the mentioned phase can form locally during the cooling of FSW nugget. This is a topic that requires more TEM studies.

The hardness profile obtained in the present work regarding the FSW of AA7075-O is different from those obtained by other researchers for the FSW of AA7075 in T6 and T7 tempers [4, 31]. The profile hardness regarding the latter is shown in Fig. 9. According to this figure, there is a minimum in hardness in HAZ. Although the hardness of SZ is much higher than that of HAZ, it is lower than the hardness of base having the maximum hardness. The SZ is completely affected while the base material is completely unaffected. Thus, the maximum hardness of the base metal is attributed to its T6 condition with the finest distribution of η' precipitates. By contrast, the HAZ and TMAZ are less affected by the generated heat. Generally speaking, the HAZ is affected only by the generated heat rather than by thermomechanical work. Consequently, the precipitates in the HAZ experience the maximum growth leading to minimum hardness due to over-aging. Leonard [4] and Linton and Ripley [1] also attributed the lowest hardness of HAZ during the FSW of AA7075-T6 to the growth and over-aging of precipitates in this region. Besides, compared to the base material, the decrease in the hardness of nugget was attributed to the partial dissolution of precipitates in the SZ [1, 4]. It is reported that such a hardness profile (Fig. 9) can be observed after annealing the heat-treatable aluminum alloys in T temper [32].

The same hardness profile obtained in the present work was also reported for AA5083-O [32]. However, the increase in the hardness of nugget in AA5083-O was attributed to the occurrence of recrystallization and in turn grain refining. As already mentioned, in case of heat-treatable aluminum alloys, the size and distribution of precipitates mostly determine and control the final properties of these alloys. By contrast, for the non-heat-treatable aluminum alloys, the grain size is the most

Table 2 Chemical composition of large precipitates based on EDS

Element	wt%	at.%
Al	16.03	31.04
Cu	81.60	67.07
Zn	2.37	1.89

Table 3 Chemical composition of small precipitates based on EDS

Element	wt%	at.%
Mg	6.50	8.58
Al	65.02	77.37
Cu	4.68	2.36
Zn	23.80	11.69

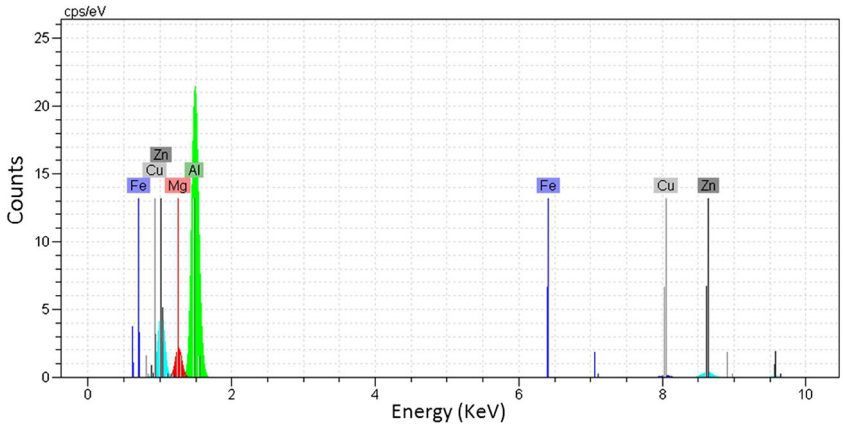

Fig. 7 EDS spectrum of the small precipitates

influential parameter in terms of strength and hardness. This was also pointed out by Guerra [33] regarding the FSW of aluminum alloys. It is reported [31] that the hardness profile of heat-treatable aluminum alloys subjected to FSW is strongly dependent on the precipitate distribution rather than on the grain size.

3.3 Tension test

The stress–strain curves obtained from the tensile testing of base metal and FSWed sample are shown in Fig. 10. The fractured specimens after tensile testing are presented in Fig. 11. According to Fig. 11, the failure occurred from the retreating side adjacent to the base metal.

Comparing the stress–strain curves presented in Fig. 10, the strength of FSWed sample is about 25 MPa higher than base metal. By contrast, the ductility of base metal is as much as twice that of FSWed case. In general, the strength of weldment of FSWed AA7075-O is higher than its base material.

Linton and Ripley [1] and Mahoney et al. [7] found that after the FSW of 7075-T651, the UTS, YS, and elongation of weldment were, respectively, about 75, 55, and 52 % of those regarding the base material. This implies that, in both works, the microstructural changes in the SZ resulted in a decrease in the strength of SZ compared to the unchanged base material. However, in the present work, the strength of SZ or weldments is higher than that of base material. As already mentioned, the increase in the strength of SZ can be attributed to breaking up the initial coarse particles to finer ones or to the solid solution and reprecipitation of particles in the SZ. However, the situation is reversed when the AA7075-T651 is subjected to FSW. In such a case, the dissolution of very fine and coherent precipitates, which are responsible for hardening/strengthening in T6 temper, results in lowering the hardness of SZ compared to its surrounding zones. In other words, the hardness of SZ is lower compared to the base material that still is in T651 condition.

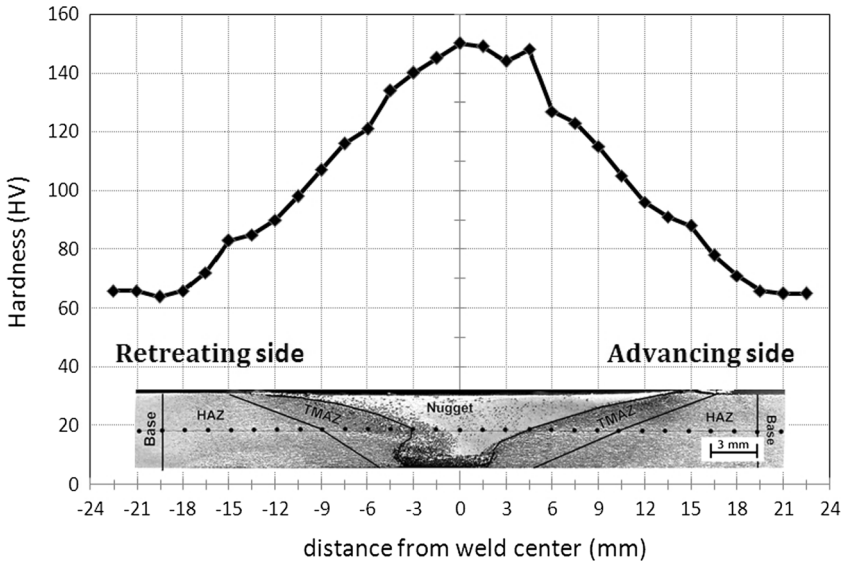

Fig. 8 Hardness profile across the weld cross section

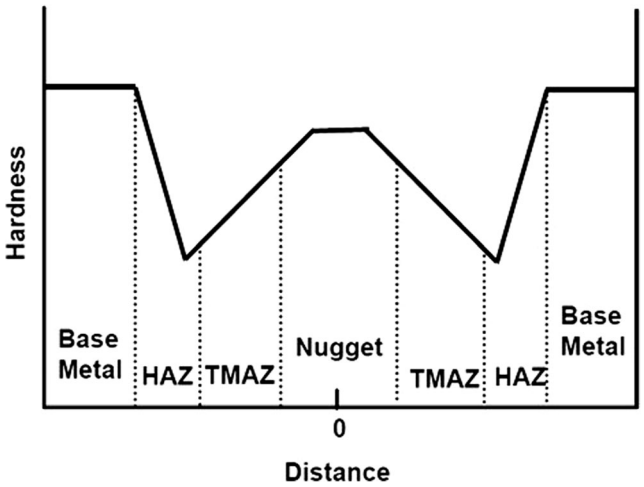

Fig. 9 The hardness profile suggested for the T6 heat-treatable aluminum alloys after subjecting to FSW [32]

In consistence with the past works [1, 7, 32], the facture in all cases occurred in the weakest region with the lowest hardness rather than in the weldment. This indicates that the welds produced by FSW are free from defects such as porosity and flaws. According to the works of Linton and Ripley [1] and Mahoney et al. [7], the fracture of FSWed AA7075-T651 took place in the HAZ whose hardness was the lowest. They attributed it to the coarse precipitates formed in the HAZ as well as to the formation of precipitation-free zone (PFZ). In the present work, as the base metal has the lowest amount of hardness (Fig. 8), the failure therefore occurred adjacent to the base metal.

3.4 Bending test

Figure 12 illustrates the curves obtained from the bending tests carried out on the base metal and FSWed specimens.

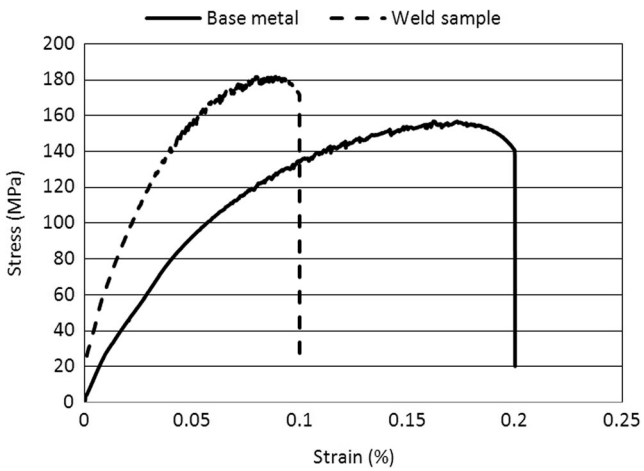

Fig. 10 Stress–strain curves of the FSWed sample compared to that of base material

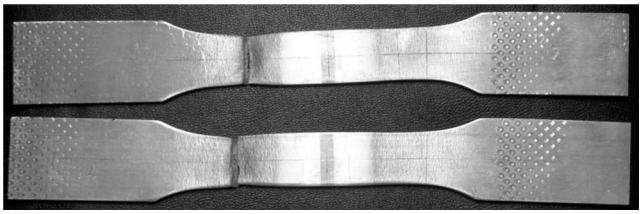

Fig. 11 Failure location in the weld tension test

According to Fig. 12, it is interesting that the results of weld face bending and weld root bending are identical, whereas there is a big difference between the results of bending carried out on base metal and weld face/weld root. This implies that compared to the conventional welding, the FSW is a unique technique in producing a more homogenous structure after welding.

The bending results are in agreement with the results of tension and hardness, i.e., the highest hardness and the lowest ductility are pertaining to weldment or SZ. In other words, the displacement or extension of SZ specimen is much lower than that of base metal. This resulted in the formation of cracks in the specimens prepared from weldment, while there was no sign of crack in the bent base metal (Fig. 13). This implies the much lower bending resistance of weldment/SZ compared to base material. Consequently, the cracks were observed in the welded specimens. One reason for such a behavior can be the difference in the precipitate size and distribution which determines the hardness or strength of AA7075. In many cases, the increase in strength is accompanied by a decrease in ductility. The fine precipitates distributed uniformly in the nugget zone prevents the dislocation mobility resulting in a pronounced decrease in the ductility.

According to Fig. 13, the FSWed specimens exhibited significant damage or cracking. However, the weld root bending showed more severe damage compared to the weld face case so that the complete separation was observed in case of

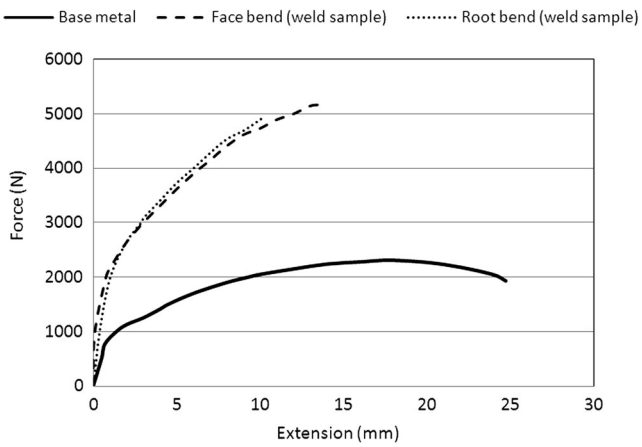

Fig. 12 Bending force vs. extension curves of the weld (root and face) compared with the base material

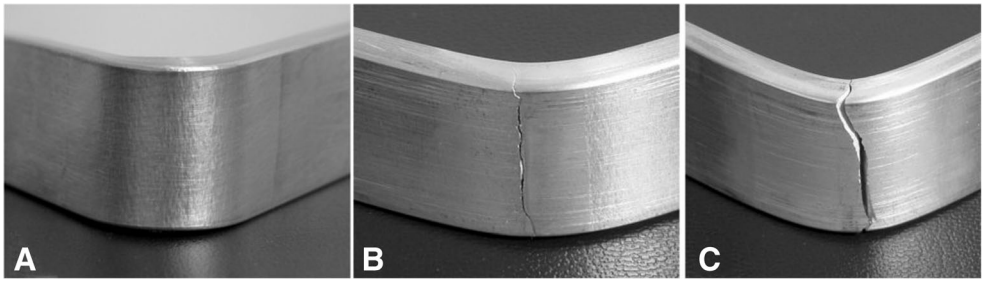

Fig. 13 Bending samples **a** base metal, **b** weld face bending, and **c** weld root bending

former. It is suggested that the bending test can be used as a criterion for flexibility and even toughness [34, 35]. Therefore, according to the results of bending tests, the FSW of AA7075-O led to a loss in toughness though the strength was increased. The detrimental effect of FSWed specimens regarding the toughness can be attributed to the changes in the characteristics of precipitates in SZ, which was already discussed.

In brief, the novelty of this works is related to this point that, according to our findings, the parts should be welded when they are in O temper but not in T6 temper. That is because when the AA7075 is welded in T6 temper, the alloy loses the strength provided by aging. In other words, welding of AA7075-T6 is deleterious to its mechanical properties by losing its strength. The situation is reversed in case of AA7075-O. Thus, this is the novelty of present work. As for the applications of AA7075-O and AA7075-T6, both have the same applications. The main applications of AA7075 alloy are in aircraft parts and structural components where high strength and good resistance to corrosion are required. As mentioned above, the parts are formed in O temper, and then, they are then aged and used in T6 temper. Regarding the weldability of AA7075-O and AA7075-T6, as their composition is the same and the only difference is in their strength, it is believed that their weldability is almost the same. However, as pointed out above, the point is that after welding, their properties are completely different. However, some may believe that AA7075-O is easier to weld, more likely because of its lower hardness/strength.

4 Conclusions

1. There are microstructural evolutions including the variations in the size and distribution of precipitates or second phases after FSW. The precipitates are relatively coarser in the HAZ and finer in the stirred zone.
2. The hardness and strength of SZ were increased at the expense of its ductility. The maximum hardness was pertaining to SZ while the base material exhibited the lowest hardness/strength. This is opposite to the results of AA7075-T6 subjected to FSW.
3. The strength of weldment of FSWed AA7075-O is higher than its base material. The increase in the strength of SZ can be attributed to breaking up the initial coarse particles to finer ones or to the solid solution and reprecipitation of particles in the SZ. In consistence with the past works, the fracture in all cases occurred in the weakest region with the lowest hardness rather than from weldment. This indicates that the welds produced by FSW are free from defects such as porosity and flaws.
4. In the bending test, the displacement amount of SZ specimen is much lower than that of base metal. This resulted in the formation of cracks in the specimens prepared from weldment, while there was no sign of crack in the base metal after bending. Thus, the crack resistance of base metal was much higher than that of weldment. This can be due to the changes in the precipitation characteristics in the SZ compared to those in base metal.

Acknowledgments The authors are thankful to Gholamreza Gordani and Behzad Adelimoghaddam for their technical assistance and valuable comments regarding this work.

References

1. Linton VM, Ripley MI (2008) Influence of time on residual stresses in friction stir welds in agehardenable 7xxx aluminium alloys. Acta Mater 56:4319
2. Paglia CS, Buchheit RG (2008) A look in the corrosion of aluminum alloy friction stir welds. Scr Mater 58:383
3. Leonard AJ (2001) Corrosion resistance of friction stir welds in aluminium alloys 2014A-T651 and 7075-T651. 3rd *Friction Stir Welding Symposium*, Kobe (Japan), TWI
4. Leonard AJ (2000) Microstructure and ageing behaviour of FSWs in aluminium alloys 2014AT651 and 7075-T651. 2nd Friction *Stir Welding Symposium*, Gothenburg (Sweden), TWI
5. Feng AH, Chen DL, Ma ZY (2010) Microstructure and cyclic deformation behavior of a friction-stir-welded 7075 Al alloy. Metall Mater Trans A. doi:10.1007/s11661-009-0152-3
6. Su JQ, Nelson TW, Sterling CJ (2005) Microstructure evolution during FSW/FSP of high strength aluminum alloys material. Sci Eng 405A:277
7. Mahoney MW, Rhodes CG, Flintoff JC, Spurling RA, Bingel WH (1998) Properties of friction-stir welded 7075 T651 aluminum. Metall Mater Trans A 29A:1955

8. Venugopal T, Srinivasa Rao K, Prasad Rao K (2004) Studies on friction stir welded AA 7075 aluminum alloy. Trans Indian Inst Metals 57:659
9. DIN standard No. 50123, Tensile test on welded joints. DIN handbook (1985). Vol. 8, welding 1, DIN. Dt. Inst. Fur Normung e. v., 2nd edition, 349–351
10. DIN standard No. 50121, Technological bending test on welded joints and weld platings. DIN handbook (1985), vol. 8, Welding 1, DIN. Dt. Inst. Fur Normung e. v., 2nd edition, 325–333
11. Koster WP, Aluminum alloys. ASM handbook (1992), vol. 9. Metallography and microstructure. The ASM Handbook Committee, ASM International, 9th edition, 351–388
12. Starink MJ, Li XM (2003) A model for the electrical conductivity of peak aged and overaged Al-Zn-Mg-Cu Alloys. Metall Mater Trans A 34A:899
13. Hadjadj L, Amira R (2009) The effect of Cu addition on the precipitation and redissolution in Al–Zn–Mg alloy by the differential dilatometry. J Alloys Compd 484:891
14. Sepold G, Kreimeyer M (2003) Joining of dissimilar materials. *Proc. of the First International Symposium on High-Power Laser Macroprocessing*, Washington, USA, 526
15. Derry CG, Robson JD (2008) Characterisation and modelling of toughness in 6013-T6 aerospace aluminium alloy friction stir welds. *Mater Sci Eng A* Vol. xxx, xxx
16. Surekha K et al (2009) Effect of processing parameters on the corrosion behaviour of friction stir processed AA 2219 aluminum alloy. Solid State Sci 11:907
17. Feng AH, Ma ZY (2007) Enhanced mechanical properties of Mg–Al–Zn cast alloy via friction stir processing. Scr Mater 56:397
18. Amirizad M et al (2006) Evaluation of microstructure and mechanical properties in friction stir welded A356+15 %SiCp cast composite. Mater Lett 60:565
19. Thomas WM, Nicholas ED (1997) Friction stir welding for the transportation industries. Mater Des 18:269
20. Ma ZY et al (2008) Microstructural refinement and property enhancement of cast light alloys via friction stir processing. Scr Mater 58:361
21. Sutton MA et al (2003) Mixed mode I/II fracture of 2024-T3 friction stir welds. Eng Fract Mech 70:2215
22. Uzun H (2007) Friction stir welding of SiC particulate reinforced AA2124 aluminium alloy matrix composite. Mater Des 28:1440
23. Mehranfar M, Dehghani K (2011) Producing nanostructured super-austenitic steels by friction stir processing. Mater Sci Eng A 528:3404
24. Bussu G, Irving PE (2003) The role of residual stress and heat affected zone properties on fatigue crack propagation in friction stir welded 2024-T351 aluminium joints. Int J Fatigue 25:77
25. Starink MJ, Deschamps A, Wang SC (2008) The strength of friction stir welded and friction stir processed aluminium alloys. Scr Mater 58:377
26. Mishra RS, Ma ZY (2005) Friction stir welding and processing. Mater Sci Eng 50R:1
27. Dehghani K, Chabok A (2011) Formation of nanograin in IF steels by friction stir processing. Mater Sci Eng A. doi:10.1016/j.msea.2011.02.069
28. Rooy EL (1992) Introduction to aluminum and aluminum alloys. ASM handbook, vol. 2. Properties and selection—nonferrous alloys and special purpose materials. The ASM Committee, 10th edition, 3–123
29. Sha G, Cerezo A (2004) Early-stage precipitation in Al–Zn–Mg–Cu alloy (7050). Acta Mater 52:4503
30. Dehghani K, Nekahi A (2010) Optimizing the bake hardening behavior of Al7075 using response surface methodology. Mater Des 31:1768
31. Genevois C, Deschamps A, Denquin A, Cottignies BD (2005) Quantitative investigation of precipitation and mechanical behaviour for AA2024 friction stir welds. Acta Mater 53:2447
32. Khaled T (2005) An outsider looks at friction stir welding. Federal aviation administration, Lakewood
33. Guerra MR (2001) Material transport during friction stir welding. *M.Sc. Thesis*, University of Texas at El Paso, USA
34. Wei S, Hao C, Chen J (2007) Study of friction stir welding of 01420 aluminum–lithium alloy. Mater Sci Eng A 452:170–177
35. Scialpi A (2007) Influence of shoulder geometry on microstructure and mechanical properties of friction stir welded 6082 aluminium alloy. Mater Des 28:1124